AN ADAPTIVE METHOD WITH RIGOROUS ERROR CONTROL FOR THE HAMILTON-JACOBI EQUATIONS. PART I: THE ONE-DIMENSIONAL STEADY STATE CASE

By

Bernardo Cockburn

and

Bayram Yenikaya

IMA Preprint Series # 1993

(September 2004)

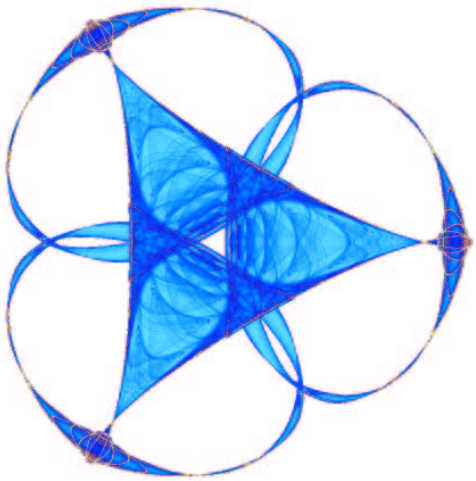

INSTITUTE FOR MATHEMATICS AND ITS APPLICATIONS

UNIVERSITY OF MINNESOTA

514 Vincent Hall

206 Church Street S.E.

Minneapolis, Minnesota 55455–0436

Phone: 612/624-6066 Fax: 612/626-7370

URL: http://www.ima.umn.edu

An adaptive method with rigorous error control for the Hamilton-Jacobi equations. Part I: The one-dimensional steady state case

Bernardo Cockburn [a,1,*], Bayram Yenikaya [a,1]

[a] *School of Mathematics, University of Minnesota, 206 Church Street S.E., Minneapolis, MN 55455, USA.*

Abstract

In this paper, we introduce a new adaptive method for finding approximations for Hamilton-Jacobi equations whose L^∞-distance to the viscosity solution is no bigger than a prescribed tolerance. This is done on the simple setting of a one-dimensional model problem with periodic boundary conditions. We consider this to be a stepping stone towards the more challenging goal of contructing such methods for general Hamilton-Jacobi equations. The method proceeds as follows. On any given grid, the approximate solution is computed by using a well known monotone scheme; then, the quality of the approximation is tested by using an approximate a posteriori error estimate. If the error is bigger than the prescribed tolerance, a new grid is computed by solving a differential equation whose devising is the main contribution of the paper. A thorough numerical study of the method is performed which shows that rigorous error control is achieved, even though only an approximate a posteriori error estimate is used; the method is thus reliable. Furthermore, the numerical study also shows that the method is efficient and that it has an optimal computational complexity. These properties are independent of the value of the tolerance. Finally, we provide extensive numerical evidence indicating that the adaptive method converges to an approximate solution that can be characterized solely in terms of the tolerance, the artificial viscosity of the monotone scheme and the exact solution.

Key words: adaptivity, a posteriori error estimates, Hamilton-Jacobi equations

* Corresponding author.
Email addresses: cockburn@math.umn.edu (Bernardo Cockburn), yenikaya@math.umn.edu (Bayram Yenikaya).

[1] Partially supported by the National Science Foundation (Grant DMS-0107609) and by the University of Minnesota Supercomputer Institute.

1 Introduction

In this paper, dedicated to Joseph E. Flaherty on the occasion of his 60 $^{\text{th}}$ birthday, we introduce and numerically study an adaptive method for approximating the *viscosity* solution of the following model steady state Hamilton-Jacobi equation

$$u + H(u_x) = f \qquad \text{in } (0,1), \tag{1}$$

with *periodic* boundary conditions. For any given positive parameter τ, the method obtains an approximation u_h satisfying the quality constraint

$$\| u - u_h \|_{L^\infty(G_h)} := \max_{i=1,\ldots,m} | (u - u_h)(y_i) | \leq \tau, \tag{2}$$

where $G_h = \{ y_i \}_{i=1}^m$ is the grid on which the approximate solution is computed. Moreover, the method achieves this with *optimal* complexity.

Let us illustrate the performance of the adaptive method for the case

$$H(p) = \frac{p^2}{\pi^2} \quad \text{and} \quad f(x) = -| \cos(\pi\, x) | + \sin^2(\pi\, x).$$

This case is particularly difficult due to the presence of a kink at $x = 1/2$ in the viscosity solution,

$$u(x) = -| \cos(\pi\, x) |.$$

The results of the first few steps of the method with a tolerance $\tau = 0.1$ are displayed in Fig. 1, where we plot the viscosity solution and its approximation.

In the first step, we take a coarse, uniform grid of 15 elements. Although the approximation is not particularly good – the error is 3.75 times the tolerance – the results of this initialization still give us valuable information to carry out the next step. Thus, we compute another uniform grid that turns out to have 47 intervals. As a consequence, the approximation error is now only 30% bigger than the tolerance. In the third step, the grid has now 61 intervals and shows signs of adapting itself to the main features of the exact solution. Indeed, we can see that it has been refined around the kink and around regions of higher convexity of the viscosity solution. Moreover, not only the approximation error is now 5% smaller than the tolerance but the distance between the approximation and the viscosity solution varies very little in all the domain. The steps could have been stopped here but we show an additional step to display the performance of the method. In this last step, the grid, with 67 intervals, is refined in a small interval containing the kink and is unrefined around it. The error increased in a neighborhood of the kink and the variation of the error across the domain became even smaller. Strict error control is maintained as the approximation error is now only 2% smaller than the tolerance.

To the knowledge of the authors, there is no other adaptive method for

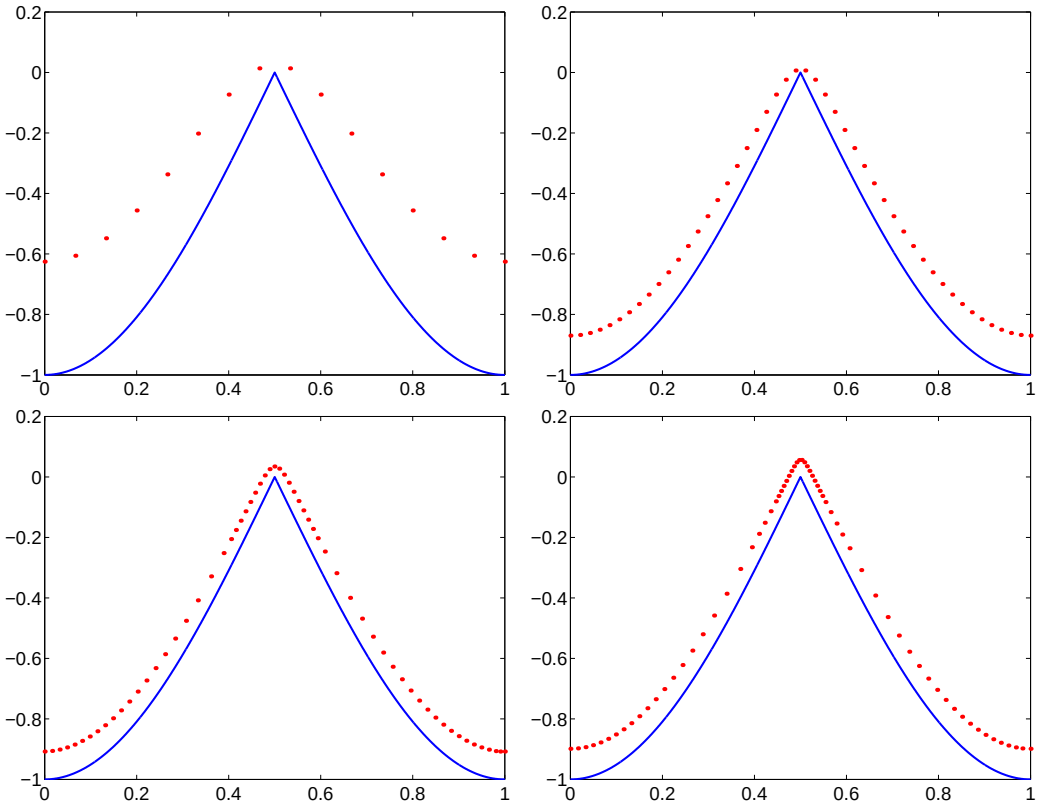

Fig. 1. Viscosity solution (solid line) and its approximation (dots): First (top, left), second (top, right), third (bottom, left) and fourth (bottom, right) steps.

Hamilton-Jacobi equations. One reason might be that a posteriori error estimates in the L^∞-norm were only recently introduced. Indeed, the adaptive method we propose uses an approximate version of the rigorous a posteriori error estimate obtained in [1], namely,

$$\| u - u_h \|_{L^\infty(0,1)} \leq \Phi(u_h),$$

where Φ is a suitably defined non-linear functional; see a similar result in [2] for the time-dependent case. A posteriori error estimates in L^1-like norms for time-dependent Hamilton-Jacobi equation with strictly convex Hamiltonians were obtained in [3, Corollary 2.2]. However, we are not aware of any adaptive method based on them.

On the other hand, there has been considerable amount of work on a posteriori error estimation and adaptive methods for scalar hyperbolic conservation laws, which are equations closely related to the Hamilton-Jacobi equations; for example, the derivative of the viscosity solution of equation (1) is the *entropy* solution of the equation

$$v + (H(v))_x = f_x.$$

A posteriori error estimates for the scalar hyperbolic conservation laws have been obtained in almost all papers concerned with error estimation for these

equations; see a review in [4]. However, only in [5] one can find a computational study of the corresponding effectivity index which is the ratio of the upper bound of the error given by the a posteriori error estimate to the actual value of the error. It was carried out for the Engquist-Osher scheme on uniform grids for the equation

$$v_t + (H(v))_x = 0.$$

The effectivity index was shown to remain very close to the ideal value of one in two cases: When the entropy solution is smooth, and when it has a discontinuity and the Hamiltonian H is linear. Unfortunately, no results were given for the difficult case in which H is a non-linear function and the entropy solution has a discontinuity. This case, however, was successfully treated by the adaptive algorithm developed in [6] where a few numerical tests show that the effectivity index is of order one. The study of the adaptive algorithm proposed in [7], does not include a study of the effectivity index. In [8], an adaptive method for a shock-capturing discontinuous Galerkin method is considered and a study of two effectivity indexes carried out for functionals of the solution of *linear* hyperbolic conservation laws. In this paper, we also carry out a thorough study of the effectivity index of our method extending in this way the work carried out in [1] for the case of uniform grids. We also display extensive numerical evidence that shows that it is reasonable to believe that the adaptive method converges to an approximate solution that can be characterized solely in terms of the tolerance τ, the artificial viscosity of the monotone scheme and the exact solution. The authors are not aware of any other similar result.

The paper is organized as follows. In Section 2, we describe in detail each of the main features of the method, namely,

(i) The use of a monotone scheme to compute the approximate solution u_h associated to any given grid G_h.
(ii) The use of an approximate a posteriori error estimate Φ_h to *try* to enforce a rigorous error control.
(iii) The use of a suitable defined *ordinary differential* equation to define a new grid. This equation is defined in terms of the previous grid, the approximate a posteriori error estimate on the corresponding approximate solution, $\Phi_h(u_h)$, and the tolerance τ.

Then, in Section 3, we carry out a thorough numerical study of its performance on five different test problems. The test problems are chosen to ensure that both the simplest as well as the most difficult cases are considered. Finally, in Section 4 we end with some concluding remarks.

2 The adaptive method

In this section, after giving a precise definition of the exact solution we seek to approximate, namely, the viscosity solution of the equation (1), we describe our adaptive method.

Given a tolerance $\tau > 0$, the method has the following form:

(0) Construct an initial grid G_h.
(1) Compute an approximate solution u_h on the grid G_h.
(2) If $\Phi_h(u_h) \leq \tau$ and the grid G_h is *reasonable*, **stop**.
(3) Otherwise, compute a new grid G_h, and go to (1).

In what follows, we describe the numerical method that we use to compute the approximate solution, the approximate a posteriori error estimate $\Phi_h(u_h)$, what do we mean by a *reasonable* grid, and, most important, how do we compute a new grid. To end, we summarize this information into a precise description of the adaptive method.

2.1 The viscosity solution

To state the definition of the viscosity solution of (1), we need the notion of *semi-differentials* of a function. The *super-differential* of a function u at a point x, $D^+u(x)$, is the set of all vectors p in $\mathbb{R}$ such that

$$\limsup_{y \to x} \left(\frac{u(y) - \{u(x) + (y-x) \cdot p\}}{|\, y - x \,|} \right) \leq 0,$$

and the *sub-differential* of a u at a point x, $D^-u(x)$, is the set of all vectors p in $\mathbb{R}$ such that

$$\liminf_{y \to x} \left(\frac{u(y) - \{u(x) + (y-x) \cdot p\}}{|\, y - x \,|} \right) \geq 0.$$

We also need to define the following quantity:

$$R(u; x, p) = u(x) + H(p) - f(x),$$

which is just the residual of u at x if $p = \nabla u(x)$.

We are now ready to define the viscosity solution of (1).

Definition 2.1 (The viscosity solution [9]) *A viscosity solution of the Hamilton-Jacobi equation* (1) *is a continuous periodic function on* $\mathbb{R}$ *such that, for all* x

in $\mathbb{R}$,

$$+R(u;x,p) \leq 0 \quad \forall p \in D^+u(x), \qquad \textit{and} \qquad -R(u;x,p) \leq 0 \quad \forall p \in D^-u(x).$$

The viscosity solution exists, for example, when both the Hamiltonian H and the right-hand side f are Lipschitz. See [9] and the references therein for more general results.

2.2 A monotone scheme

Given a grid $G_h = \{ x_i \}_{i=1}^n$, where the point $x_n = 1$ is always identified with the point $x_0 := 0$ because of the periodicity of the problem, we take the approximate solution u_h to be a piecewise linear function with value $u_{h\,j}$ at the grid-point x_j. We determine these values by using the following monotone scheme:

$$u_{h\,j} + H\left(\frac{z_{j+1/2} + z_{j-1/2}}{2}\right) - \omega\left(z_{j+1/2} - z_{j-1/2}\right) = f(x_j), \tag{3}$$

$$z_{j+1/2} = \frac{u_{h\,j+1} - u_{h\,j}}{x_{j+1} - x_j}, \tag{4}$$

$$\omega = \sup_{p \in \mathcal{R}(f)} |\, H'(p) \,|, \tag{5}$$

where

$$\mathcal{R}(f) = \left[\inf_{\delta>0}\inf_{x\in\mathbb{R}}\left(\frac{f(x+\delta)-f(x)}{\delta}\right), \sup_{\delta>0}\sup_{x\in\mathbb{R}}\left(\frac{f(x+\delta)-f(x)}{\delta}\right)\right].$$

Notice that in the above expression, we can take $x \in \mathbb{R}$ since f is periodic.

The existence and uniqueness of the approximate solution can be obtained by a fixed-point argument; see, for example, [10]. A simple modification of the proof for monotone schemes for the time-dependent monotone schemes obtained in [11] can be used to prove that its approximate solution also converges to the viscosity solution as the maximum grid-size

$$\Delta x = \max_{j=0,\ldots,n-1} (x_{j+1} - x_j),$$

goes to zero.

The viscosity parameter ω is taken as in (5) to ensure the monotonicity of the method. Indeed, a simple calculation shows that such property is verified provided that

$$\omega \geq \max_{j=0,\ldots,n-1} \left| H'\left(\frac{z_{j+1/2} + z_{j-1/2}}{2}\right) \right|.$$

Since in such a case, we also have that

$$\mathcal{R}(u_h) \subset \mathcal{R}(f),$$

the choice (5) does ensure the monotonicity of the method and, moreover, allows us to compute the parameter ω in terms of the data of the problem. Motivated by the fact that a smaller ω results in better approximations to the kinks of the viscosity solution, and by the fact that

$$\mathcal{R}(u) \subset \mathcal{R}(f),$$

we took the viscosity coefficient as follows:

$$\omega = \sup_{p \in \mathcal{R}(u)} | H'(p) |.$$

This choice also seems to ensure the monotonicity of the scheme. This is the parameter we use in all our numerical experiments.

2.3 The approximate a posteriori error estimate

In this subsection, we present the rigorous and then the approximate a posteriori error estimates obtained in [1]. To do so, we need to introduce several quantities. First, we introduce the following semi-norms:

$$| u - v |_- = \sup_{x \in \Omega} (u(x) - v(x))^+, \qquad | u - v |_+ = \sup_{x \in \Omega} (v(x) - u(x))^+,$$

where $w^+ \equiv \max\{0, w\}$ and $\Omega = \mathbb{R}$.

Next, we consider the following generalization of the residual:

$$R_\epsilon(u; x, p) = u(x) + H(p) - f(x - \epsilon\, p) - \frac{1}{2}\epsilon\, | p |^2, \tag{6}$$

which is called the *shifted residual*.

Finally, we introduce the paraboloid P_v,

$$P_v(x, p, \kappa; y) = v(x) + (y - x) \cdot p + \frac{\kappa}{2} | y - x |^2 \qquad y \in \mathbb{R}, \tag{7}$$

where x is a point in $\mathbb{R}$, p is a vector of $\mathbb{R}$, and κ is a real number.

We are now ready to state the a posteriori error estimate.

Theorem 2.2 (A posteriori error estimate [1]) *Let u be the viscosity solution of the equation* (1) *and let v be any continuous function on $\mathbb{R}$ periodic*

with period 1. *Then, for* $\sigma \in \{-,+\}$, *we have that*

$$| u - v |_\sigma \le \inf_{\epsilon \ge 0} \Phi_\sigma(v;\epsilon), \tag{8}$$

where

$$\Phi_\sigma(v;\epsilon) = \sup_{(x,p)\in\mathcal{A}_\sigma(v;\epsilon)} \Big(\sigma\, R_{\sigma\epsilon}(v;x,p)\Big)^+. \tag{9}$$

The set $\mathcal{A}_\sigma(v;\epsilon)$ *is the set of elements* (x,p) *satisfying*

$$\begin{aligned} &x \in \mathbb{R}, \\ &p \in D^\sigma v(x), \\ &\sigma\,\{v(y) - P_v(x,p,\sigma/\epsilon\,;\,y)\} \le 0 \qquad \forall y \in \mathbb{R}. \end{aligned}$$

(For $\epsilon = 0$, *only the first two conditions apply.)*

Note that the above result implies that

$$\| u - v \|_{L^\infty(\Omega)} \le \Phi(v),$$

where

$$\Phi(v) = \max\left\{\inf_{\epsilon\ge 0} \Phi_+(v,\epsilon), \inf_{\epsilon\ge 0} \Phi_-(v,\epsilon)\right\}.$$

In practice, we do not use the above functional Φ, but an approximation Φ_h, also introduced in [1]. The functional Φ_h is given by

$$\Phi_h(v) = \max\left\{\inf_{\epsilon\in\mathcal{E}_h} \Phi_{h,+}(v,\epsilon), \inf_{\epsilon\in\mathcal{E}_h} \Phi_{h,-}(v,\epsilon)\right\}.$$

Let us describe the set $\mathcal{E}_h$. Instead of taking the parameter ϵ in the interval $[0,\infty)$, we take it in the discrete set $\mathcal{E}_h$, where

$$\mathcal{E}_h = \{i \cdot E/N, 0 \le i \le N\},$$

where

$$E = 2\,E_0\,\Delta x\,\omega\,|\,\ln(1/\Delta x\,\omega)\,| \quad \text{and} \qquad N = 4\,|\,\ln(1/\Delta x\,\omega)\,|.$$

Here ω is the artificial diffusion coefficient defined by (5).

We pick E_0 in an adaptive way. Following [1], we first take $E_0 = 1$. If neither the first nor the last element in $\mathcal{E}_h$ is picked as the optimal ϵ, we consider that our choice of E_0 was reasonable. If instead the first element E/N is picked as the optimal ϵ, we set $E_0 := E_0/N$ and start anew. Finally, if the last element E is picked as the optimal ϵ, then we set $E_0 := E_0 \cdot N$ and restart.

It remains to describe the functional $\Phi_{h,\sigma}(v,\epsilon)$. These functionals are obtained from the functional $\Phi_\sigma(v,\epsilon)$ by simply replacing the set $\mathcal{A}_\sigma(v;\epsilon)$ by the set $\mathcal{A}_{h,\sigma}(v;\epsilon)$ which is defined as the set of elements (x,p) satisfying

$x \in \Omega_h$,
$p \in D^\sigma v(x)$,
$\sigma \{v(y) - P_v(x, p, \sigma/\epsilon\,;\, y)\} \le 0 \qquad \forall y \in \Omega_h : |\, y - x \,| \le 2 \,\|\, v \,\|_{Lip(\Omega)}\, \epsilon,$

where

$$\Omega_h = \mathbb{Z} + \left\{ x_{j+1/2} := (x_j + x_{j+1})/2 \right\}_{j=0}^{n-1}.$$

Note that when $v = u_h$ and $x = x_{j+1/2}$, we have

$$p = u_h'(x_{j+1/2}) = \frac{u_{h\,j+1} - u_{h\,j}}{x_{j+1} - x_j},$$

and hence we have a very simple way to compute the shifted residual. Note also that if we replace Ω_h by Ω, the above test is *equivalent* to the original test in Theorem 2.2; see [1].

2.4 Computing a new grid

To describe the way we compute a new grid, we need to introduce an auxiliary mapping that associates a grid of the domain $[0, 1)$ to any given bounded and integrable function $\Gamma : (0, 1) \to \mathbb{R}^+$. It is defined as follows. First, we solve the equation

$$\frac{1}{\Gamma}\,\frac{d}{dx}\mathcal{N} = 1 \quad \text{ in } (0,1), \quad \text{ where } \mathcal{N}(0) = 0. \tag{10}$$

Then, we set

$$\mathcal{G}(\Gamma) = \{\, x_j = \mathcal{N}^{-1}(j) \,\}_{j=1}^{n},$$

where n is the smallest natural number greater or equal to $\mathcal{N}(1)$.

Let us give two examples to illustrate the action of this mapping. First, consider the case in which the function Γ is the constant function m. Then, since

$$\mathcal{N}(x) = \int_0^x \Gamma(s)\, ds = m\, x,$$

the grid $\mathcal{G}(\Gamma)$ is nothing but the *uniform* grid $\{\, x_j = j/m \,\}_{j=1}^{m}$.

Now, take Γ to be the inverse of the grid-size function of the grid $G_h = \{\, y_i \,\}_{i=1}^{m}$, that is, of the function

$$h(y) = y_{i+1} - y_i \quad \text{ for } y \in (y_i, y_{i+1}), \qquad i = 0, \cdots, m.$$

Then, the grid $\mathcal{G}(\Gamma)$ in nothing but the *original* grid G_h itself since we have

$$\mathcal{N}(y_i) = \int_0^{y_i} \Gamma(s)\, ds = \sum_{j=0}^{i-1} \int_{y_j}^{y_{j+1}} \frac{1}{y_{j+1} - y_j}\, dx = i \quad \text{ for } i = 0, \cdots, m.$$

In other words, the grid-size function of the grid $\mathcal{G}(1/h)$ is nothing but h itself.

This simple fact suggests a way of using the above mapping to compute a new grid given the grid-size function of an old one. Indeed, if we take $\Gamma = \mu/h$, $\mathcal{G}(\Gamma)$ is a grid whose grid-size function is, roughly speaking, $1/\Gamma = h/\mu$. Thus, the new grid will be refined or unrefined according to whether the function μ is bigger or smaller than one, respectively. Hence, we take this *grid-size modification* function μ to depend on the ratio of the approximate a posteriori error estimate to the tolerance. Indeed, if the approximate a posteriori error estimate is bigger than the tolerance, we need to refine the grid and hence μ should be bigger than one. If, on the other hand, the approximate a posteriori error estimate is smaller than the tolerance, we need to unrefine the grid in order to optimize our computational resources; in this case μ should be smaller than one. For this reason, we take

$$\mu := \Psi(\gamma),$$

where γ captures the information of the ratio between the approximate a posteriori error estimate and the tolerance, and Ψ is a function which tells us how much refinement or unrefinement we are to do for a given value of γ.

The function γ is taken as follows:

$$\gamma(s) = \frac{1}{\tau} \min \Big\{ \max_{|\ell - j| \leq 2} | \, R(u_h; x_{\ell+1/2}, u_h'(x_{\ell+1/2})) \, |, \Phi_h(u_h) \Big\}, \tag{11}$$

for $s \in (x_j, x_{j+1})$ where $j = 0, \cdots, n-1$. If we simply take γ to be a constant function equal to $\Phi_h(u_h)/\tau$, since $\Phi_h(u_h)$ is only an upper bound for the error, this choice could result in unnecessarily over-refined grids. It is much better to take into account the variations of the residual over the computational domain. Finally, note that we have taken the maximum of the residual in five points to take into account the fact that the residual at a given point $x_{j+1/2}$ actually depends on the values of the approximate solution at the points x_{j-1}, x_j, x_{j+1}, and x_{j+2}.

The function Ψ is defined as follows:

$$\Psi(g) = \begin{cases} g\,(1 + \sqrt{g-1}), & g > 1, \\ \frac{g+3}{4}, & 0 \leq g \leq 1 \end{cases}$$

First, note that $\Psi(1) = 1$. This means that if γ is identically equal to one, which implies that the quality constraint is satisfied, the grid-modification function $\mu = \Psi(\Gamma)$ will also be identically equal to one. Also, note that Ψ is an increasing function. This implies that when γ is less than one, then $\mu = \Psi(\Gamma)$ will also be less than one, as expected. A similar property holds if γ is bigger than one.

We arrived to the above form for Ψ after extensive experimentation. We began by taking the simple choice of $\Psi(g) = g$. The numerical results we carried out, not reported here, indicated that around regions when the residual is actually equal to zero, the adaptive method was *unrefining too much*. In other words, if $g \in (0, 1)$, the choice $\Psi(g) = g$ was giving too small a number. In order to reduce the amount of unrefinement requested by the method, we took $\Psi(g) = (g + 3)/4$.

To further reduce the tendency towards unrefinement, we take

$$\mu := \max\{1, \Psi(\gamma)\},$$

whenever we consider that our grid is *reasonable*, that is, whenever we have that

$$\| (1 - \Psi(\gamma))^+ \|_{L^1(0,1)} \leq 0.02.$$

Let us give an interpretation of the above inequality. Note that if at some point of the domain we have $(1 - \Psi(\gamma))^+ > 0$, the adaptive method will try to unrefine around that point. The inequality above states that even if certain amount of unrefinement is unfulfilled, we consider our grid to be reasonable. Also, note that it is simply unreasonable to have the left hand side equal to zero. Indeed, consider the case for which residual is zero at some points of the domain. Since around those points we can almost certainly have that $\Psi(\gamma) < 1$, we are always going to try to unrefine the grid around those points. Typically, this results in excessive unrefinement, which is then compensated with refinement, but only to be once again followed by more unrefinement. To break these limit cycles, we *only refine* if the above inequality is satisfied.

After these modifications, our experiments indicated that the convergence of the adaptive method was still extremely slow. This happened because, when the maximum of the function γ was very close to one, the method was *not refining enough*. In order to increase the amount of refinement when $g \geq 1$, especially when $g \approx 1$, we replaced $\Psi(g) = g$ by $\Psi(g) = g(1 + \sqrt{g - 1})$.

Let us end the discussion of the construction of the function Ψ by pointing out that our numerical experiments did not provide any indication that would led us to believe that its form might actually depend on the data of the problems, namely, the Hamiltonian H and the right-hand side f.

2.5 The adaptive method

We are now ready to describe in a precise way our adaptive method.

Given a tolerance $\tau > 0$, the method computes an approximation u_h to the viscosity solution of (1) as follows:

(0) Set $G_h = \{\, j/15 \,\}_{j=1}^{15}$.

(1) Compute the approximate solution u_h by using a monotone method on the grid G_h. Then, compute the approximate a posteriori error estimate $\Phi_h(u_h)$ and the function $\Psi(\gamma)$.

(2) If

$$\Phi_h(u_h) \leq 1 \quad \text{and} \quad \| \, (1 - \Psi(\gamma))^+ \, \|_{L^1(0,1)} \leq 0.02,$$

stop.

(3) Otherwise, compute the grid-size function h, the grid-modification function μ, the new grid $G_h = \mathcal{G}(h/\mu)$, and go to (1). The first new grid is the uniform grid $G_h = \{\, j/n \,\}_{j=1}^{n}$, where n is the smallest natural number greater or equal to $\mathcal{N}(1)$.

Using a uniform grid for the first new grid improves the quality of the grids obtained by the algorithm. It does not, however, alter the convergence properties of the method.

3 Numerical Results

3.1 The test problems.

We test our adaptive method on the very same problems used in [1] for the study of the approximate a posteriori error estimate we are using; see Table 1. Note that the short names given in that table are used throughout this section to refer to a particular problem. The first letter(s) refers to the type of the Hamiltonian, and the last letter(s) refer to smoothness of the exact solution. For example, **CNS** refers to the problem with convex Hamiltonian and non-smooth solution.

This set of problems has the advantage of having the three main types of Hamiltonians, namely, linear, strictly convex or concave, and non-convex. Also, the solutions of the first three problems are smooth whereas those of the last two problems have a kink at $x = 1/2$. We can thus be confident that our adaptive method should perform on any other problem (1) in the way it performed in the test problems we consider.

3.2 Results with the adaptive method

Here we display and discuss the results obtained by applying the adaptive method. The tolerance τ takes the values of 10^{-2}, 10^{-3} and 10^{-4}.

Table 1
The test problems.

Short Name	Hamiltonian $H(p)$	right-hand side $f(x)$	viscosity solution $u(x)$
CS	$-p^2/4\pi^2$ (concave)	$\cos^4(\pi\, x)$	$\cos^2(\pi\, x)$
NCS	$p^3/8\pi^3$ (non-convex)	$\sin(2\pi x) + \cos^3(2\pi x)$	$\sin(2\pi x)$
LS	p (linear)	$\cos^2(\pi\, x) - \pi \sin(2\pi\, x)$	$\cos^2(\pi\, x)$
CNS	p^2/π^2 (convex)	$-\mid \cos(\pi\, x)\mid + \sin^2(\pi\, x)$	$-\mid \cos(\pi\, x)\mid$
NCNS	$-p^4 + 2p^2 - 1$ (non − convex)	$u(x) + H(u'(x))$ if $x \neq 1/2$	$\begin{cases} x^2, \text{ if } 0 \leq x \leq \frac{1}{2}, \\ (x-1)^2, \text{ if } \frac{1}{2} \leq x \leq 1. \end{cases}$

In Table 2, we can see that the method enforces a strict control on the error $\| u - u_h \|_{L^\infty(G_h)}$ since the effectivity index

$$ei_\tau(\tau; u, u_h) = \frac{\tau}{\| u - u_h \|_{L^\infty(G_h)}},$$

is always bigger than one; the adaptive method is thus reliable. We can also see that the effectivity index

$$ei_{adap}(\tau; u_h) = \frac{\tau}{\Phi_h(u_h)},$$

which is a measure of the quality of the adaptive method, is remarkably close to the ideal value of one, independently of the huge variations in the value of the tolerance. More than that, in Figs. 2 and 3, for $\tau = 10^{-3}$ and $\tau = 10^{-4}$, respectively, we see that modification function $\Psi(\gamma)$, whose maximum is precisely $\Phi_h(u_h)$, is very close to be *identically* equal to 1. Thus, the adaptive method is extremely efficient.

Of course, this efficiency refers only to the last step of the adaptive algorithm. To have an idea of the efficiency of the whole adaptive method, we must compare the computational complexity needed to carry out all the steps of the method with the computational complexity needed to carry out the last one. Since in our case, the complexity of each step is proportional to the number of elements of the grid, our measure of efficiency is the complexity ratio

$$cmplxr = \frac{\sum_{k=1}^{K} n^k}{n^K},$$

where n^k is the number of intervals of the grid of the step k, and K is the number of steps needed for convergence. A bigger complexity ratio indicates a

less efficient adaptive method. In the last two columns of Table 2, we display the numbers of steps needed for convergence and the complexity ratio. We see that the complexity ratio, which is always less that five, is essentially equal to the number of steps minus one. Since the initial step involves the computation on a grid of only 15 points, it is reasonable to expect that this step would not have an impact in the overall computational complexity of the algorithm. Hence, the adaptive method converges with an *optimal* complexity, that is, with only a few times the complexity needed to carry out its last step.

Table 2
History of convergence of the adaptive method.

Problem	τ	n	$\| u - u_h \|_{L^\infty(G_h)}$	order	$ei_\tau(\tau; u, v)$	$ei_{adap}(\tau; v)$	steps	$cmplxr$
CS	1.0E-2	212	9.93E-3	–	1.01	1.00	6	4.88
	1.0E-3	2040	9.98E-4	1.01	1.00	1.00	4	2.77
	1.0E-4	20071	1.00E-4	1.01	1.00	1.00	6	4.78
NCS	1.0E-2	1301	9.36E-3	–	1.07	1.01	5	3.54
	1.0E-3	12320	9.87E-4	1.00	1.01	1.00	5	3.58
	1.0E-4	120749	9.98E-5	1.00	1.00	1.00	4	2.61
LS	1.0E-2	1271	2.35E-3	–	4.26	1.00	4	2.89
	1.0E-3	12587	2.42E-4	0.99	4.13	1.00	5	3.89
	1.0E-4	125690	2.44E-5	1.00	4.10	1.00	5	3.89
CNS	1.0E-2	454	9.95E-3	–	1.01	1.00	3	2.05
	1.0E-3	4085	9.98E-4	1.05	1.00	1.00	3	2.13
	1.0E-4	40148	9.99E-5	1.01	1.00	1.00	5	4.15
NCNS	1.0E-2	357	9.97E-3	–	1.00	1.00	4	2.73
	1.0E-3	3378	9.97E-4	1.02	1.00	1.00	4	2.74
	1.0E-4	32458	9.99E-5	1.02	1.00	1.00	4	2.80

It is interesting to note that the effectivity index

$$ei_h(u, u_h) = \frac{\Phi_h(u_h)}{\| u - u_h \|_{L^\infty(G_h)}}$$

for the adaptive grids does not behave exactly as it did for the uniform grids. Indeed, noting that

$$ei_h(u, u_h) = ei_\tau(\tau; u, u_h)/ei_{adap}(\tau, u_h) \approx ei_\tau(\tau; u, u_h),$$

from Tables 2 and 3, we see that although there is no significant difference in the cases of non-linear Hamiltonians and smooth solutions, in the case of a linear Hamiltonian with a smooth case, the effectivity index for the adaptive

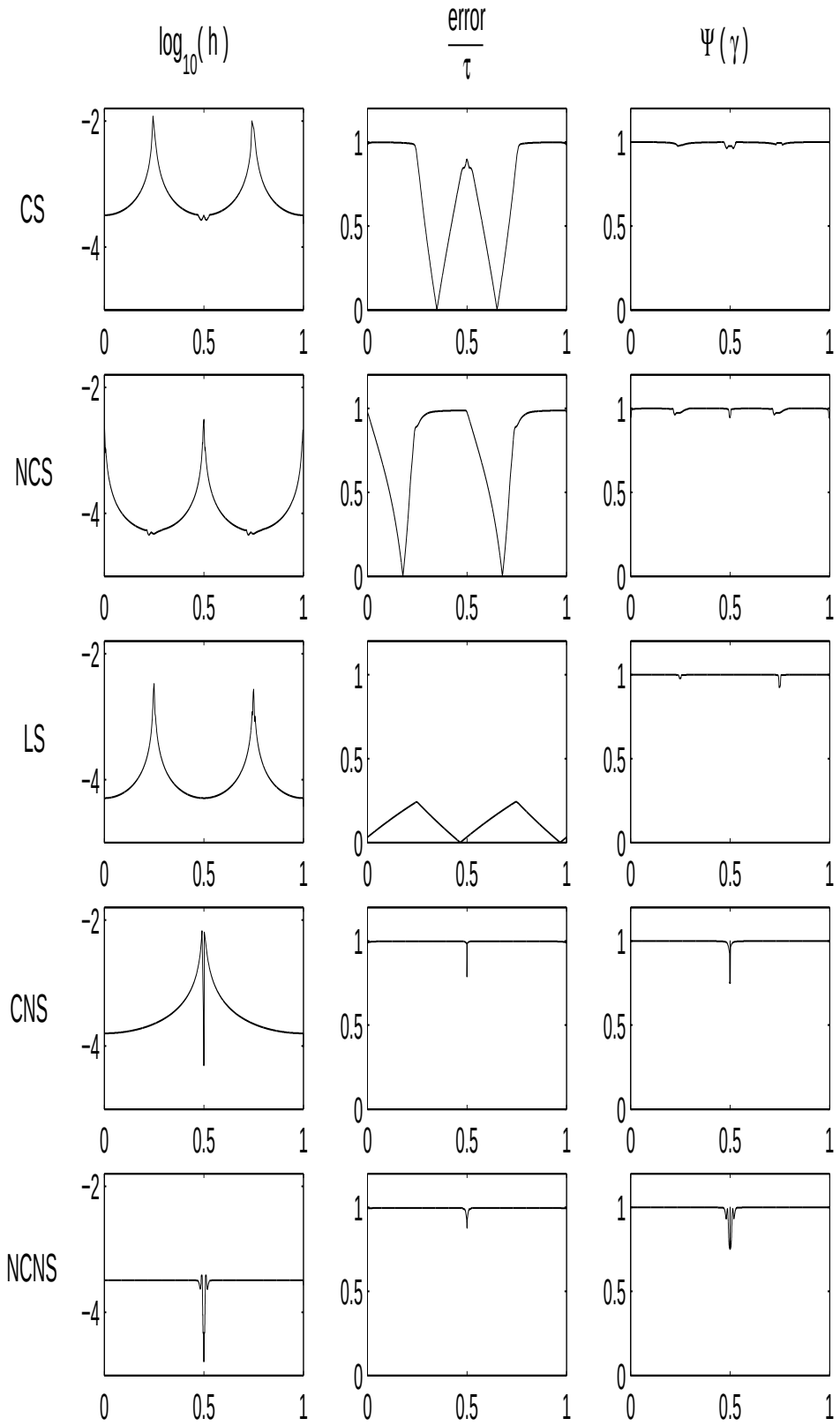

Fig. 2. Convergence step, $\tau = 10^{-3}$.

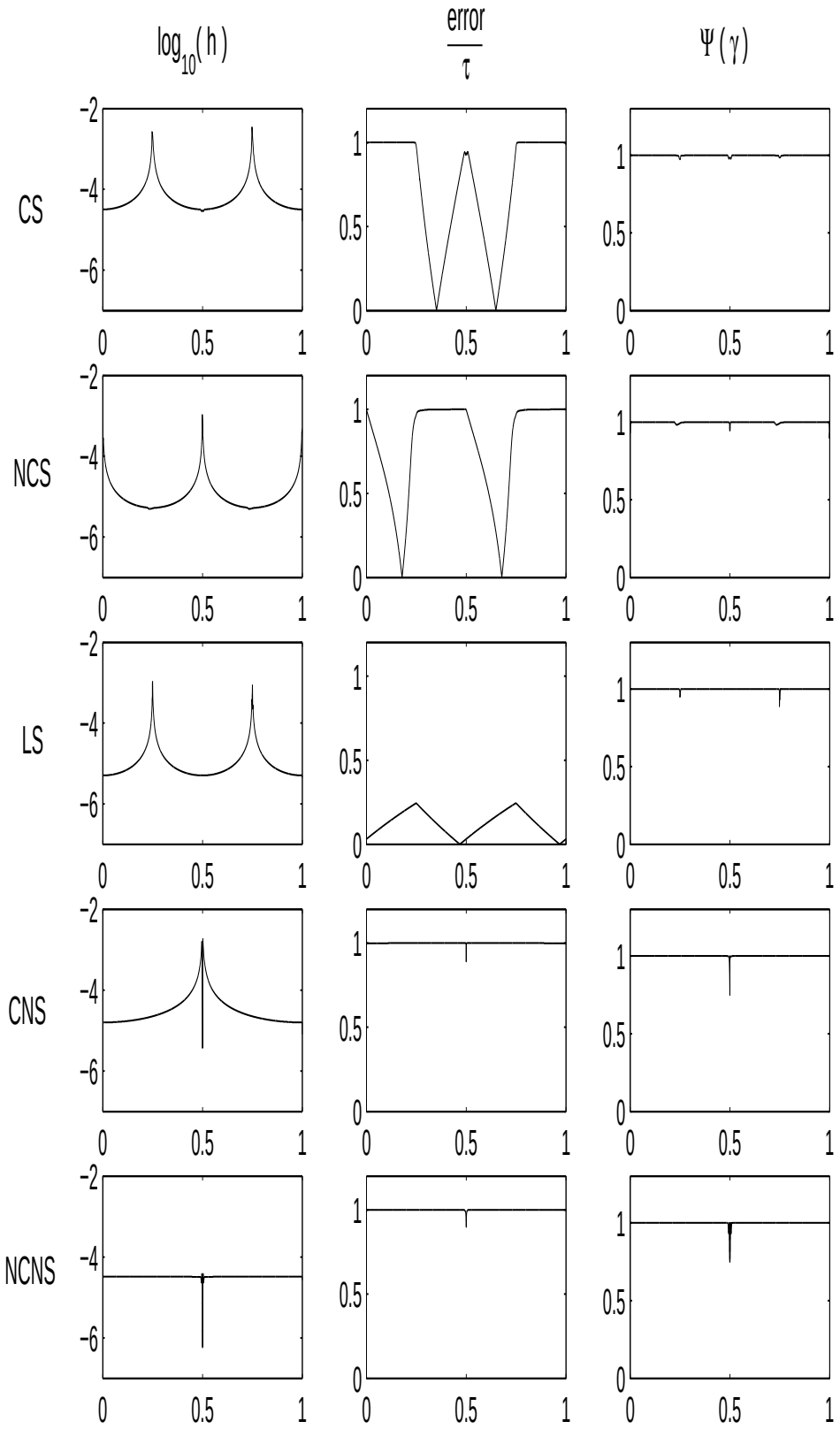

Fig. 3. Convergence step, $\tau = 10^{-4}$.

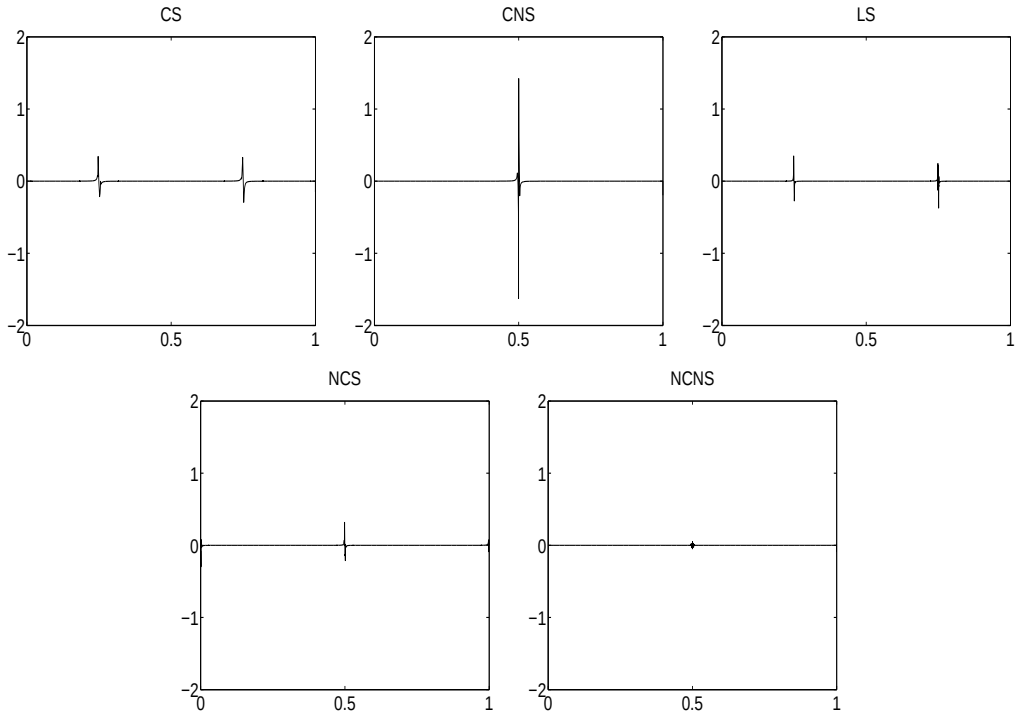

Fig. 4. Quality of the adaptive grid: Logarithm of the ratio of the lengths of successive intervals in the final grid.

grids is about $4/6.36 \approx 0.63$ times smaller than that for the uniform grids. In the case of non-linear Hamiltonians and non-smooth viscosity solutions, the difference is even more remarkable. Indeed, from Tables 2 and 4 we can see that for the adaptive grids, the effectivity index remains essentially equal to one as the error in the approximation varies from 10^{-2} to 10^{-4}, whereas for the uniform grids, the index increases from ≈ 2.4 to ≈ 4.5 when the Hamiltonian is convex, and from ≈ 3.3 to ≈ 13 when the Hamiltonian is non-convex. The refinement strategy of the adaptive method around the kink might be responsible for this behavior.

Finally, let us point out that the grids produced by the method are very smooth in most of the domain. Indeed, in Fig. 4, we display *logaritm* of the ratio of the size of two consecutive intervals. We can see that it is essentially equal to *zero* in most of the domain.

3.3 The approximate solution obtained by the adaptive method

In this subsection, we present numerical evidence suggesting that the adaptive method converges to an approximation that can be characterized in terms of the viscosity coefficient of the tolerance τ, the numerical method ω and the viscosity solution u.

Table 3
History of convergence for uniform grids: Smooth solution test problems.

Problem	n	$\| u - u_h \|_{L^\infty(G_h)}$	order	$ei_h(u, u_h)$
CS	40	7.4E-2	–	1.02
	80	3.8E-2	0.96	1.01
	160	1.9E-2	0.98	1.00
	320	9.8E-3	0.99	1.00
	640	4.9E-3	1.00	1.00
	1280	2.5E-3	1.00	1.00
	2560	1.2E-3	1.00	1.00
	5120	6.1E-4	1.00	1.00
	10240	3.1E-4	1.00	1.00
	20480	1.5E-4	1.00	1.00
	40960	7.7E-5	1.00	1.00
NCS	40	3.1E-1	–	1.39
	80	1.8E-1	0.81	1.42
	160	9.8E-2	0.86	1.34
	320	5.2E-2	0.90	1.24
	640	2.7E-2	0.93	1.14
	1280	1.4E-2	0.96	1.08
	2560	7.2E-3	0.97	1.03
	5120	3.6E-3	0.98	1.01
	10240	1.8E-3	0.99	1.00
	20480	9.2E-4	1.00	1.00
	40960	4.6E-4	1.00	1.00
LS	40	7.5E-2	–	6.38
	80	3.8E-2	0.97	6.37
	160	1.9E-2	0.99	6.37
	320	9.7E-3	0.99	6.36
	640	4.8E-3	1.00	6.36
	1280	2.4E-3	1.00	6.36
	2560	1.2E-3	1.00	6.36
	5120	6.1E-4	1.00	6.36
	10240	3.0E-4	1.00	6.36
	20480	1.5E-4	1.00	6.36
	40960	7.6E-5	1.00	6.36

Indeed, we claim that such an approximation is the approximate solution obtained by the monotone scheme for the grid given by

$$\mathcal{G}(\omega \,|\, u'' \,|/\tau),$$

Table 4
History of convergence for uniform grids: Non-smooth solution test problems.

Problem	n	$\| u - u_h \|_{L^\infty(G_h)}$	order	$ei_h(u, u_h)$
CNS	40	1.5E-1	–	1.69
	80	7.7E-2	0.98	1.69
	160	3.9E-2	0.99	1.96
	320	2.0E-2	0.99	2.31
	640	9.8E-3	1.00	2.43
	1280	4.9E-3	1.00	2.89
	2560	2.5E-3	1.00	3.03
	5120	1.2E-3	1.00	3.45
	10240	6.1E-4	1.00	3.77
	20480	3.1E-4	1.00	4.02
	40960	1.5E-4	1.00	4.58
NCNS	40	7.7E-2	–	1.56
	80	3.8E-2	1.00	1.96
	160	1.9E-2	1.00	2.51
	320	9.6E-3	1.00	3.27
	640	4.8E-3	1.00	4.31
	1280	2.4E-3	1.00	5.19
	2560	1.2E-3	1.00	6.65
	5120	6.0E-4	1.00	8.74
	10240	3.0E-4	1.00	10.83
	20480	1.5E-4	1.00	13.77
	40960	7.5E-5	1.00	17.27

when the viscosity solution is smooth. Recall that this grid is given by

$$\{\, \mathcal{N}^{-1}(j) \,\}_{j=1}^{n},$$

where

$$\mathcal{N}(x) = \frac{\omega}{\tau} \int_0^x |u''(s)|\, ds.$$

For the case in which the viscosity solution has a kink at $x = 1/2$, we use the following modification

$$\mathcal{N}(x) = \begin{cases} \frac{\omega}{\tau} \int_0^x |u''(s)|\, ds, & \text{if} \quad 0 \le x < 1/2, \\ \frac{\omega}{\tau} \int_0^{1/2} |u''(s)|\, ds + \frac{\omega}{\tau} \int_{1/2}^x |u''(s)|\, ds & \text{if } 1/2 < x \le 1. \end{cases}$$

The results in Fig. 5 support this claim. Therein, we compare the grid-size function of the above grid, which we call the *optimal* grid, with that of the grid obtained with the adaptive method for $\tau = 10^{-4}$. We see that they are almost identical for all the problems. Moreover, we can see that the grids are more refined whenever the absolute value of the second order derivate of the

viscosity solution, when defined, is bigger and that the peaks in the grid-size functions, which correspond to the biggest mesh-size, of the first four problems occur at the points at which the second derivative of the viscosity solution is equal to zero. Note that in the last problem, the second derivative of the approximate solution is *constant*, except at the point $x = 1/2$. This results in a grid which is uniform except in a small neighborhood around the kink. For the two last problems, the grid is more refined around the kinks. In all the cases, the grid obtained by the adaptive algorithm is slightly more refined than the optimal grid, as we can see in the last column of Fig. 5.

Next, we provide a heuristic argument that shows that in fact this is not such an unexpected occurrence. Let us consider the case in which the viscosity solution is actually smooth. Then, the optimal grid would satisfy the identity

$$\tau = | R(u_h) |.$$

If we *replace* the residual by the truncation error, we get

$$\tau = | TE(u) | \approx \omega | u'' | h,$$

and hence,

$$1/h \approx \omega | u'' |/\tau.$$

This means that $\mathcal{G}(\omega | u'' |/\tau)$ should provide us with the wanted grid. In the case in which the viscosity solution has a kink, the above heuristic reasoning holds except for a few consecutive intervals containing the kink. Thus, if we use the above formula for $\mathcal{N}$, we still should get reasonable results.

3.4 Adaptivity versus uniform refinement

In this subsection, we compare the efficiency of computing in uniform grids and that of computing in the non-uniform grid resulting from our adaptive method. We do that in two ways. First, by taking the exact error $\| u - u_h \|_{L^\infty(0,1)}$ as the measure of quality of the approximation and then the approximate a posteriori error estimate $\Phi_h(u_h)$.

We begin by considering the exact error. In Fig. 6, we plot the history of convergence for both methods. We see that for convex Hamiltonians, the computation with adaptive grids is more efficient than that for uniform ones. We also see that for the linear Hamiltonian, there is essentially no difference. Finally, in the case of non-convex Hamiltonians, we see that using adaptive grids is clearly more efficient when the solution is smooth. In the non-smooth case computation with the uniform grid seems to be slightly more efficient but the advantage disappears as the tolerance goes to zero. This happens because in

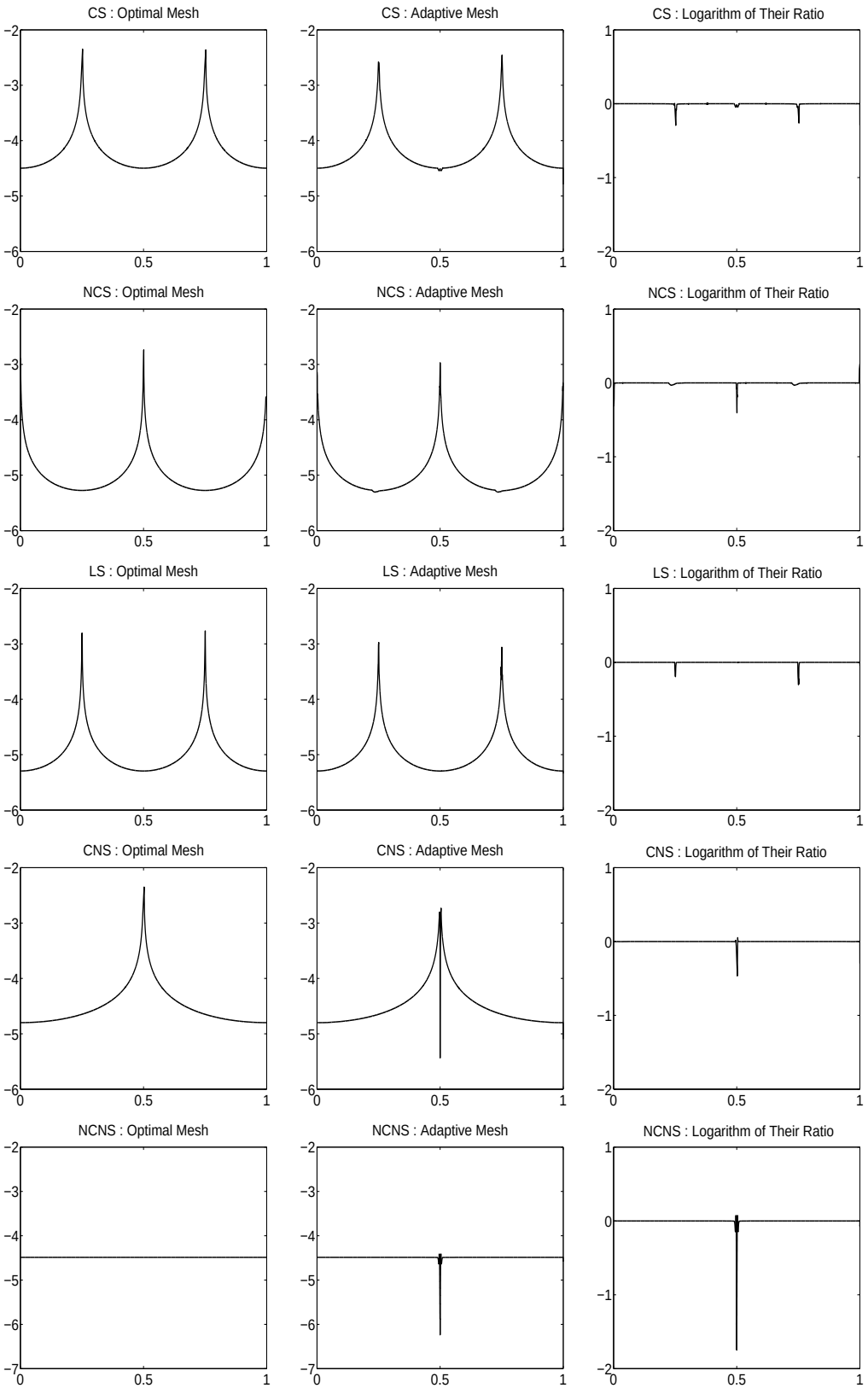

Fig. 5. Optimal and adaptive grid-size functions for $\tau = 10^{-4}$.

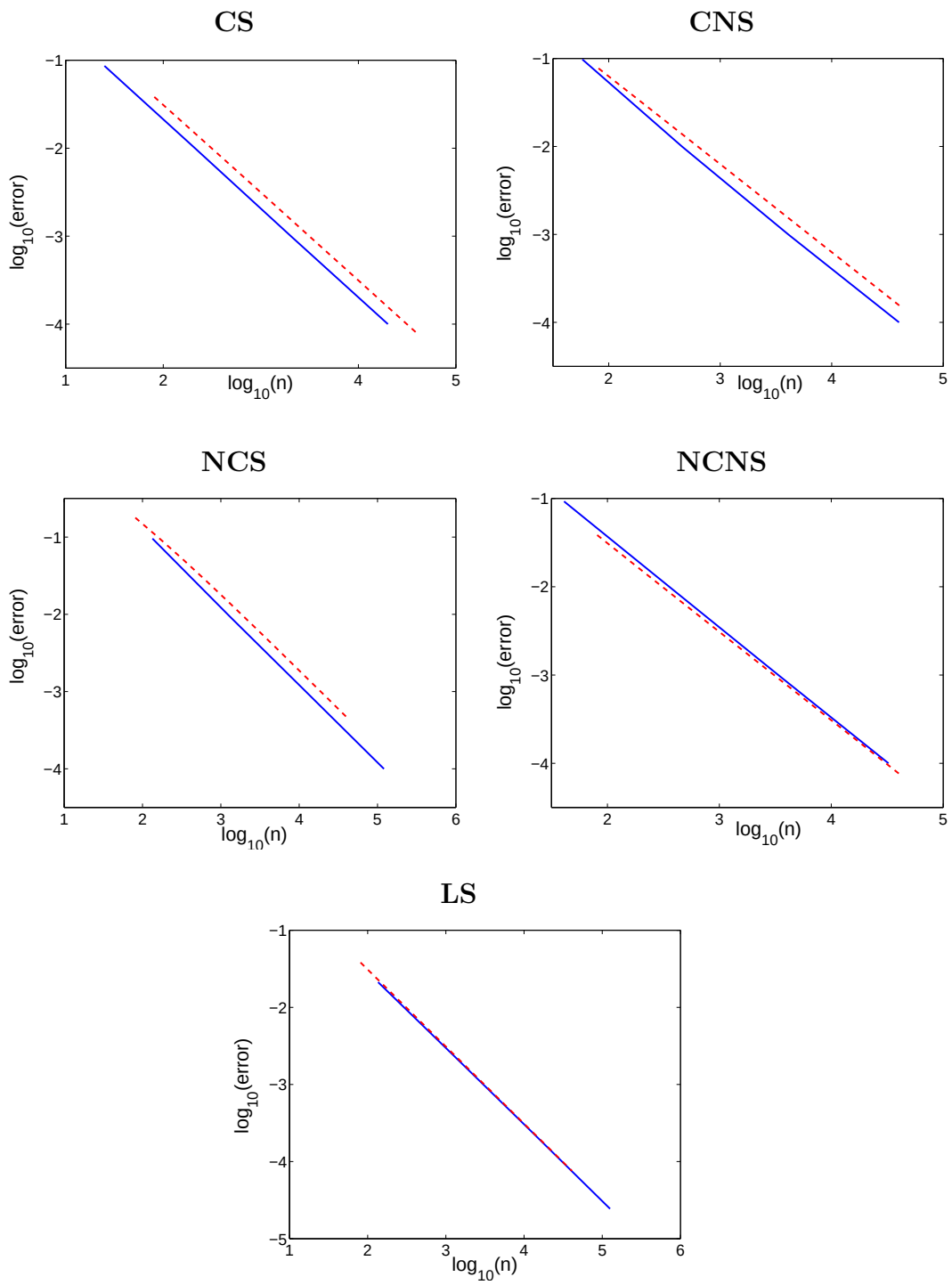

Fig. 6. Comparison of convergence rates: Uniform (dashed line) and adaptive (solid line) refinement.

this case, the adaptive grid is actually a uniform grid except for a very small region around the kink; see Figs. 2 and 3.

Next, we take as our measure of quality the a posteriori error estimate $\Phi_h(u_h)$

since this is the only quantity we can actually compute if we do not know the viscosity solution. Making use of the heuristic argument proposed in the previous subsection, we should have that

$$n_{unif} = \frac{\omega}{\Phi_h(u_h)} \| u'' \|_{L^\infty(0,1)} \quad \text{and} \quad n_{adap} = \frac{\omega}{\Phi_h(u_h)} \| u'' \|_{L^1(0,1)},$$

when the viscosity solution is smooth. In Table 5, obtained from Tables 3 and 2, we can see numerical evidence that supports this claim. Hence, in such a case we see that

$$\frac{n_{unif}}{n_{adap}} = \frac{\| u'' \|_{L^\infty(0,1)}}{\| u'' \|_{L^1(0,1)}} \geq 1.$$

This means that computing the approximate solution with the adaptive grid is *always* more efficient that computing it with the uniform grid that produces the same value of $\Phi(u_h)$. In each of the three problems with smooth solutions, we have that the above ratio is equal to $\pi/2 \approx 1.57$. Hence, in these cases, computing in a uniform grid is about 57% more costly than computing in the adaptive grid for the same value of $\Phi(u_h)$.

Table 5
Behavior of $n \cdot \Phi_h(u_h)$ for adaptive and uniform grids.

Problem	$\Phi_h(u_h)$	$n_{adap} \cdot \Phi_h(u_h)/(\omega \cdot \| u'' \|_{L^1(0,1)})$	$\Phi_h(u_h)$	$n_{unif} \cdot \Phi_h(u_h)/(\omega \cdot \| u'' \|_{L^\infty(0,1)})$
CS	1.0E-2	1.06	9.8E-3	1.00
	1.0E-3	1.02	1.2E-3	0.98
	1.0E-4	1.00	1.5E-4	0.98
NCS	9.9E-3	1.07	1.5E-2	1.01
	1.0E-3	1.02	1.8E-3	0.98
	1.0E-4	1.01	4.6E-4	1.00
LS	1.0E-2	1.01	3.1E-2	0.99
	1.0E-3	1.00	1.9E-3	0.99
	1.0E-4	1.00	4.8E-4	1.00

For the cases in which the viscosity solution is not smooth, that is, for the last two problems, we cannot use the above approach. Instead, we simply plot, in Fig. 7, the number of intervals of the grid versus the corresponding $\Phi_h(u_h)$. We see that the advantage of using an adaptive grid is much more accentuated in this case than in the case in which the viscosity solution is smooth.

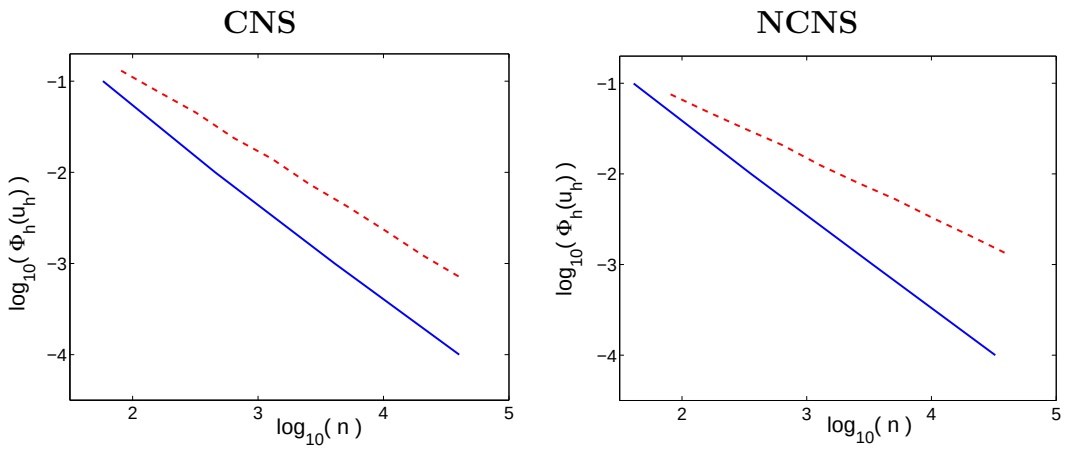

Fig. 7. Comparison of convergence rates: Uniform (dashed line) and adaptive (solid line) refinement.

4 Conclusions, extensions and on-going work

In this paper, we have proposed an adaptive method for computing approximations to the viscosity solution of a model steady state Hamilton-Jacobi equation. The method has been shown to exert a rigorous error control and to be extremely reliable and efficient for a wide variation of the tolerance parameter even in the presence of kinks in the viscosity solution. Moreover, we have provided numerical evidence that supports a characterization of the approximate solution given by the method in terms of the tolerance, the viscosity coefficient and the exact solution.

In the multi-dimensional case, monotone schemes, like the Lax-Friedrichs scheme and the ones introduced in [12] and in [13], can be employed. Also, the a posteriori error estimate introduced in [1], which is independent of the space dimension, can be easily used. The key point here is how to obtain a suitable extension of the mapping $\Gamma \mapsto \mathcal{N}$ with which the new grid is constructed. One possible approach is immediately suggested when we realize that the equation defining such a map, namely, equation (10), is nothing but the following *eikonal* equation:

$$\frac{1}{\Gamma}\left|\frac{d}{dx}\mathcal{N}\right| = 1 \quad \text{in } (0,1), \quad \text{where } \mathcal{N}(0) = 0.$$

Thus, in several space dimensions, we can solve the eikonal equation

$$\frac{1}{\Gamma}\,|\,\nabla\mathcal{N}\,| = 1 \quad \text{in } \Omega, \quad \text{where } \mathcal{N} = 0 \quad \text{on } \partial\Omega,$$

to define a new grid. This new approach to adaptivity is currently being studied.

In the time-dependent case, straightforward extensions of the above mentioned monotone schemes can be used. However, in this case the time-space grids must be allowed to vary locally and the schemes must be properly modified to handle them. The a posteriori error estimate obtained in [2] can be used. Although we have focused on monotone schemes, the adaptive method proposed here can be easily applied to high-order accurate methods like the discontinuous Galerkin method developed in [14]. The above extensions constitute the subject of ongoing work.

Acknowlegements. The authors would like to thank the reviewers for several remarks leading to a better presentation of the material in this paper.

References

[1] S. Albert, B. Cockburn, D. French, T. Peterson, A posteriori error estimates for general numerical methods for Hamilton-Jacobi equations. Part I: The steady state case, Math. Comp. 71 (2002) 49–76.

[2] S. Albert, B. Cockburn, D. French, T. Peterson, A posteriori error estimates for general numerical methods for Hamilton-Jacobi equations. Part II: The time-dependent case, in: R. Herbin, D. Kröner (Eds.), Finite Volumes for Complex Applications, Vol. III, Hermes Penton Science, 2002, pp. 17–24.

[3] C.-T. Lin, E. Tadmor, L^1-stability and error estimates for approximate Hamilton-Jacobi solutions, Numer. Math. 87 (2001) 701–735.

[4] B. Cockburn, Continuous dependence and error estimation for viscosity methods, Acta Numerica (2003) 127–180.

[5] B. Cockburn, H. Gau, A posteriori error estimates for general numerical methods for scalar conservation laws, Mat. Aplic. e Comp. 14 (1995) 37–45.

[6] D. Kröner, M. Ohlberger, A posteriori error estimates for upwind finite volume schemes for nonlinear conservation laws in multidimensions, Math. Comp. 69 (2000) 25–39.

[7] L. Gosse, C. Makridakis, Two a posteriori error estimates for one-dimensional scalar conservation laws, SIAM J. Numer. Anal. 38 (2000) 964–988 (electronic).

[8] E. Süli, P. Houston, Adaptive finite element approximation of hyperbolic problems, in: T. Barth, H. Deconink (Eds.), Error Estimation and Adaptive Discretization Methods in Computational Fluid Dynamics, Vol. 25 of Lecture Notes in Computational Science and Engineering, Springer Verlag, Berlin, 2002, pp. 269–344.

[9] M. Crandall, L. Evans, P.-L. Lions, Some properties of viscosity solutions of Hamilton-Jacobi equations, Trans. Amer. Math. Soc. 282 (1984) 487–502.

[10] B. Cockburn, J. Qian, Continuous dependence results for Hamilton-Jacobi equations, in: D. Estep, S. Tavener (Eds.), Collected Lectures on the Preservation os Stability under Discretization, SIAM, 2002, pp. 67–90.

[11] M. Crandall, P. Lions, Two approximations of solutions of Hamilton-Jacobi equations, Math. Comp. 43 (1984) 1–19.

[12] R. Abgrall, Numerical discretization of the first-order Hamilton-Jacobi equations on triangular meshes, Comm. Pure Appl. Math. 49 (1996) 1339–1377.

[13] G. Kossioris, C. Makridakis, P. Souganidis, Finite volume schemes for Hamilton-Jacobi equations, Numer. Math. 83 (1999) 427–442.

[14] C. Hu, C.-W. Shu, A discontinuous Galerkin finite element method for Hamilton-Jacobi equations, SIAM J. Sci. Comput. 21 (1999) 666–690.